

Enhanced Performance by Polyaniline/Tailored Carbon Nanotubes Composite as Supercapacitor Electrode Material

Tingting Ye,^{1,2} Yafei Kuang,^{1,2} Congjia Xie,^{1,2} Zhongyuan Huang,^{1,2} Changjun Zhang,^{1,2}
Dan Shan,^{1,2} Haihui Zhou^{1,2}

¹State Key Laboratory for Chemo/Biosensing and Chemometrics, Hunan University, Changsha 410082, People's Republic of China

²College of Chemistry and Chemical Engineering, Hunan University, Changsha 410082, People's Republic of China

Correspondence to: H. Zhou (E-mail: haihuizh@163.com)

ABSTRACT: Polyaniline/tailored carbon nanotubes composite (PANI/TCN) synthesized via situ polymerization of aniline monomer in the presence of tailored carbon nanotubes (TCN) is reported as electrode material for supercapacitors. The morphology, structure, and thermostability of the composite were characterized by scanning electron microscope, Fourier transform infrared, and thermogravimetric analysis. The electrochemical property of the resulting material was systematically studied using cyclic voltammetry and galvanostatic charge–discharge. The results show that the short rod-like PANI dispersed well in the TCN with three-dimensional network structure. The as-prepared composite shows high specific capacitance and good cycling stability. A specific capacitance of 373.5 F g⁻¹ at a current density of 0.5 A g⁻¹ was achieved, which is much higher than that of pure PANI (324 F g⁻¹). Meanwhile, the composite retains 61.7% capacity after 1000 cycles at a scan rate of 50 mV s⁻¹. The enhanced specific capacitance and capacity retention indicates the potential of composite as a promising supercapacitor electrode material. © 2013 Wiley Periodicals, Inc. *J. Appl. Polym. Sci.* 2014, 131, 39971.

KEYWORDS: batteries and fuel cells; conducting polymers; functionalization of polymers; nanotubes; nanoparticles; nanowires and nanocrystals

Received 19 July 2013; accepted 10 September 2013

DOI: 10.1002/app.39971

INTRODUCTION

With the aggravation of the energy crisis, energy storage/conversion devices have been intensely researched for many years.^{1–3} As an ideal energy storage device, electrochemical supercapacitors have been used in uninterrupted power supplies, mobile/portable electronic devices, micro-autonomous robots, hybrid vehicles, and distributed sensor applications,^{4–6} because of their high power density, reversibility, long cycle life, and small environmental impact.^{7–10}

As a typical electrode material of pseudocapacitors,¹¹ polyaniline (PANI) has attracted wide interests because of its excellent capacity for energy storage, easy synthesis in aqueous medium, high conductivity, good environmental stability in air, simplicity in doping, low price of aniline monomer, and ease of manipulation.^{12,13} All of these have made it to be an exceptionally versatile material with application in energy storage/conversion devices. However, swelling and shrinkage of PANI during the charge–discharge process must be considered,¹⁴ because the irreversible change of PANI has important effect on the cycle life of polymer-based capacitors. And the instability of the structure is

the most important reason why PANI cannot bear high current density during the charge–discharge process, which greatly limits the wide development of PANI in supercapacitors. On the other hand, electrical double-layer capacitors,¹⁴ such as carbon nanomaterials, have high capacitance which comes from the charge accumulation at the interface between electrode and electrolyte. Generally, carbon nanomaterials, such as activated carbons,¹⁵ carbon nanofibers,¹⁶ carbon nanotubes,¹⁷ and graphene nanosheets,¹⁸ display high surface area, high electrical conductivity, long cycle life, and good mechanical properties. High surface area can provide more electroactive regions, which is necessary for effective access of electron from the electrolyte to the electrode. And high conductivity of electroactive materials is an important factor to meet fast electron transport for the high rate charge–discharge process. Therefore, many efforts have been made in recent years to improve the electrochemical performance of PANI by modifying with carbon materials, such as graphene^{19,20} and carbon nanotubes.^{21–27} Liu et al. found that the specific capacitance of PANI was enhanced to 175 F g⁻¹ at 1 A g⁻¹ after modified by three-dimensional graphene, but the conducting potential range of the composite is still narrow.²⁰

Zhou et al. showed that polyaniline/multiwalled carbon nanotubes (MWCNTs) composite had good cycle life, which lost 29.1% of the maximum capacity after 700 cycles, whereas the specific capacitance was only 177 F g^{-1} at 5 mV s^{-1} .²³ Gupta et al. reported that the specific capacitance of the single-walled carbon nanotube coated with polyaniline could reach up to 463 F g^{-1} at 10 mA cm^{-2} and the capacitance retains 96% after 1500 cycles, however, the range of the potential is only 0.75 V .²⁴ Sivakkumar et al. reported that the specific capacitance of polyaniline/multiwalled carbon nanotube composite reached up to 606 F g^{-1} at a constant current of 1.0 A g^{-1} , and Wang et al. showed that the specific capacitance of PANI-coated buckypaper was 424 F g^{-1} at 200 mA g^{-1} , but the range of the potential were 0.4 V and 0.8 V , respectively.^{25,26} All of these show that it is not easy to obtain a PANI composite with great specific capacitance, wide range of potential and long cycle life. Generally, PANI modified by unprocessed carbon nanotubes or graphene cannot achieve appealing results. The reason is that pristine carbon nanotubes is easily intertwined and graphene is easily aggregated because of huge Van der Waals force between layers, which decreases the carbon nanomaterials' advantage of high surface area and high specific capacitance. Tailored assembly is an important way to improve the performance of carbon nanomaterials. For example, Wang et al. used selective etching in molten nitrate to cut long MWCNTs into short MWCNTs with opened ends and rough surfaces.²⁸ The lengths of the products can be controlled by the etching temperature and time. Jiao et al. reported that MWCNTs can be transversely cut into single- or few-layer graphene nanoribbons (GNRs) (20%) and multilayer GNRs or GNRs with carbon nanotubes cores (80%) by plasma etching, which have huge surface area and those peculiar morphologies are hard to aggregate.²⁹ Kosynkin et al. longitudinally unzipped carbon nanotubes to GNRs via oxidation treatment, and the results showed that MWCNTs were completely unzipped to perfect nanosheets.³⁰ They also used potassium vapor to split carbon nanotubes, high conductive nanotubes with three-dimensional network structure were obtained.³¹ Thus it can be seen that the tailored assembly of carbon nanomaterials also provides a new approach to modify conducting polymer.

In this paper, tailored carbon nanotubes (TCN), which were prepared by tailoring MWCNTs through a modified Hummers method,³² were used to modify PANI by in situ polymerization of aniline monomer in the presence of TCN. Different from the normal two-dimensional structure of carbon materials, TCN possess the unique hybrid structure of 1D nanotube and 2D graphene which not only can provide huge surface area but also greatly reduce the agglomeration of TCN. PANI modified by TCN can get amazing results different from other carbon nanomaterials. The synergic effect of PANI and TCN contributes to the better specific capacitance and stability.

EXPERIMENTAL

Materials

The raw MWCNTs (main range of diameter 60–100 nm, length 5–15 μm , purity > 97%, model: L-MWNT-60100, Shenzhen Nanotech Port) are commercially available. Aniline, ammonium

persulfate, sodium nitrate, sulfuric acid, potassium permanganate, and other chemicals and reagents used in this work are in analytical grade, which were purchased from Sinopharm Chemical Reagent, China. Ultrapure water was used for preparation, dilution, and analytical purpose.

Preparation of TCN

TCN were synthesized by a modified Hummers method, including two processes: (i) oxidizing and tailoring MWCNTs, (ii) reduction of oxidized tailored carbon nanotubes (OTCNs). In the first step, MWCNTs (1 g) and sodium nitrate (0.5 g) were put into a 250 mL round-bottomed flask, which contained 98% H_2SO_4 (46 mL), stirred for 1 h in ice-water bath. Then 3 g of KMnO_4 was gradually added with stirring and the temperature in the whole process was strict controlled under 10°C . After mixing uniformly, the temperature was kept at 35°C for 1 h. Subsequently with stirring, 46 mL of ultrapure water was slowly added. After cooling to room temperature, 30% H_2O_2 solution (12 mL) was dropped into the suspension liquid within half an hour and then diluted to 500 mL by ultrapure water. The product was filtered and washed with HCl (5 wt %) and ultrapure water for several times, respectively. After drying under vacuum, the OTCNs were obtained as gray powder.

In the second step, hydrazine monohydrate was used to reduce OTCNs to TCN. Specific operations are as follows: the OTCNs (100 mg) were dispersed in 50 mL ultrapure water by ultrasonic treatment, then, 0.1 mL of hydrazine monohydrate (85%) was added. Subsequently, the temperature was gradually increased to 95°C and the mixture was refluxed for 1 h. The reduced materials were filtered and washed with ultrapure water for several times. These materials named TCN were dried at 60°C in a vacuum oven.

Preparation of Polyaniline/Tailored Carbon Nanotubes

To get polyaniline/tailored carbon nanotubes (PANI/TCN), the following two procedures were carried out: one is combination of PANI and OTCNs, the other is reduction process similar to deoxidation of OTCNs. In the combination process, PANI was synthesized using in situ polymerization in HCl solution. First of all, aniline was distilled under vacuum to remove the oxidation impurities before it was used. 100 mg of OTCNs were dispersed in 1M HCl (50 mL) containing a certain amount of aniline (quality ratio of aniline to OTCNs varies as 2 : 8, 5 : 5 and 8 : 2) by ultrasonic treatment 1 h. While keeping vigorous stirring at room temperature, ammonium peroxydisulfate (molar ratio of aniline to ammonium peroxydisulfate is 4 : 1) in 1M HCl aqueous solution was rapidly poured into the mixture. The polymerization lasted overnight. The mixture was washed and centrifuged with ultrapure water, ethanol and hexane for several times to remove the unreacted aniline, then, dried under vacuum at 60°C . The composites were designated as PANI/OTCNs 2-8, PANI/OTCNs 5-5, and PANI/OTCNs 8-2, respectively.

For comparison, the pure polyaniline fiber was synthesized without oxidized tailored MWCNTs by the same way.

Chemical conversion of oxidized tailored carbon nanotubes in the PANI/OTCNs composite to the TCN is the reduction process

that refers to the process of deoxidation of OTCNs. After that, the materials (0.1 g) were dispersed into 20 mL of 1M HCl solution contain ammonium peroxydisulfate (0.1 g) and stirred at room temperature overnight. The products were obtained by filtration and repetitive washing with ultrapure water, ethanol and hexane. After drying at 60°C in a vacuum oven, these products named as PANI/TCN 2-8, PANI/TCN 5-5, and PANI/TCN 8-2, respectively, were obtained from the corresponding PANI/OTCNs composites.

Materials Characterization

The morphologies of the prepared samples were observed using scanning electron microscope (SEM, Hitachi S-4800, Japan). The chemical structure of materials was confirmed by recording infrared spectra on a Fourier transform infrared (FTIR) spectrophotometer (NICOLET 6700) fitted with diffuse reflectance assembly. NETZSCH-409PC thermogravimetric analyzer (TGA) was used to measure the thermal stability by heating the material from room temperature to 600°C at heating rate of 10°C min⁻¹ under a continuous flow of dry nitrogen gas.

Electrochemical Measurements

All electrochemical experiments were carried out on a CHI 760C electrochemical workstation system (Shanghai Chenhua Instrument Factory, China) using three-electrode system. Platinum filament and saturated calomel electrode were used as the counter and reference electrodes, respectively. The working electrode was prepared by dropping 1 mg mL⁻¹ electrode material solution (25 μL) which dispersed in ultrapure water onto a glassy carbon electrode with a diameter of 4 mm. The electrochemical properties of the composite, PANI and TCN were investigated by cyclic voltammetry (CV) and galvanostatic charge-discharge curves in 1M H₂SO₄ aqueous solution.

RESULTS AND DISCUSSION

Morphology and Structure

The morphologies of MWCNTs, TCN, PANI, PANI/TCN 2-8, PANI/TCN 5-5, and PANI/TCN 8-2 are shown in Figure 1. Long MWCNTs intertwined with each other in Figure 1(a), and the pure PANI was uniform short rod-like and closely packed together as shown in Figure 1(b). As shown in Figure 1(c), the TCN were partly tailored from MWCNTs, and curved like nanopipes. However, long incisions can still be seen on the nanotubes. The morphologies of PANI/TCN 2-8, PANI/TCN 5-5, and PANI/TCN 8-2 are shown in Figure 1(d-f), respectively. Less amount of PANI dispersed in intertwined carbon nanotubes as shown in Figure 1(d). In Figure 1(e), carbon nanotubes intertwined with each other, forming a three-dimensional network structure and the PANI dispersed well in it. Plenty of PANI can be seen in Figure 1(f) and partly sheltered from the three-dimensional network structure of TCN. The formation mechanism of the PANI-OTCNs composite is as follows³³: aniline was adsorbed on the surface of OTCNs with three-dimensional network structure in the process of polymerization. On addition of oxidant, polymerization proceeds both in solution (bulk polymerization) and on the surface of OTCNs. Carbon material acts as poly-

merization catalyst. However, PANI is highly agglomerated in solution phase. Therefore, polymerization proceeds at much faster rate on the surface of OTCNs than in solution phase. And effective rate of deposition of PANI on OTCNs is much faster than bulk polymerization in solution phase. The PANI-OTCNs composite with three-dimensional network structure was obtained.

The chemical structures of PANI, TCN, and PANI/TCN 8-2 materials are depicted by FTIR spectra, as shown in Figure 2. Typical peaks at 1584 and 1111 cm⁻¹ in PANI are corresponding to the quinoidal structure and much higher than the peak at 1395 cm⁻¹ that is attributed to the benzenoid structure. It means that PANI has a high doping level. The peak of PANI at 1290 cm⁻¹ relates to the C-N stretching vibration. While typical peak of N-H group is covered by high intensity absorption peak at 3434 cm⁻¹ of O-H group results from the H₂O remained in sample. The peak of C=O group at 1721 cm⁻¹ is weak in the FTIR spectra of the TCN and PANI/TCN, indicating a high degree of reduction of OTCNs. On the other hand, the intense peaks of PANI/TCN 8-2 composite at 1138 and 1588 cm⁻¹ are found owing to the quinoidal structure of PANI. The results demonstrate that PANI and TCN combined well and the composite has a high degree of doping.

The thermostability of PANI, TCN, and PANI/TCN 8-2 were tested by TGA and the results are shown in Figure 3. All materials have a little mass loss around 100°C, which is attributed to the evaporation of H₂O in the samples. TCN have a slight mass loss about 10% from 100°C to 600°C, which is presumably owing to the decomposition of some residual oxygen-containing groups.³⁴ Meanwhile, PANI exhibits a 54% mass loss between 100°C and 600°C, indicating a structural decomposition of the polymer.³⁵ The curve of the weight loss of PANI/TCN 8-2 is between those of TCN and PANI. From 100°C to 200°C, it has a slight mass loss similar to TCN, whereas it has about 17% weight loss between 200°C and 600°C owing to PANI in the composite. All of these mean that PANI/TCN 8-2 has better thermal stability with less mass loss compared with pure PANI.

Electrochemical Characterization

The CV of the materials with a potential window from -0.2 to 0.8 V are shown in Figure 4. In Figure 4(a), the CV curve of TCN is nearly rectangular in shape, indicating good charge propagation within the electrode materials. However, the CV curve of PANI is not rectangular. Two couples of redox peaks are observed from the CV curve of PANI, corresponding to redox transition of leucoemeraldine form (semiconducting state) and polaronic emeraldine form (conducting state). The CV curve of PANI shows that the electrode reaction current is nearly 0 from -0.2 to 0 V in the positive scan. Nevertheless, the CV curve of PANI modified by TCN represents good symmetry that is analogous to that of TCN. Compared with the CV curves of various materials measured at the same condition, it is not difficult to find that PANI/TCN 8-2 is the better ratio among the composite materials. Meanwhile, PANI/TCN 8-2 composite exhibits higher anodic current and cathodic

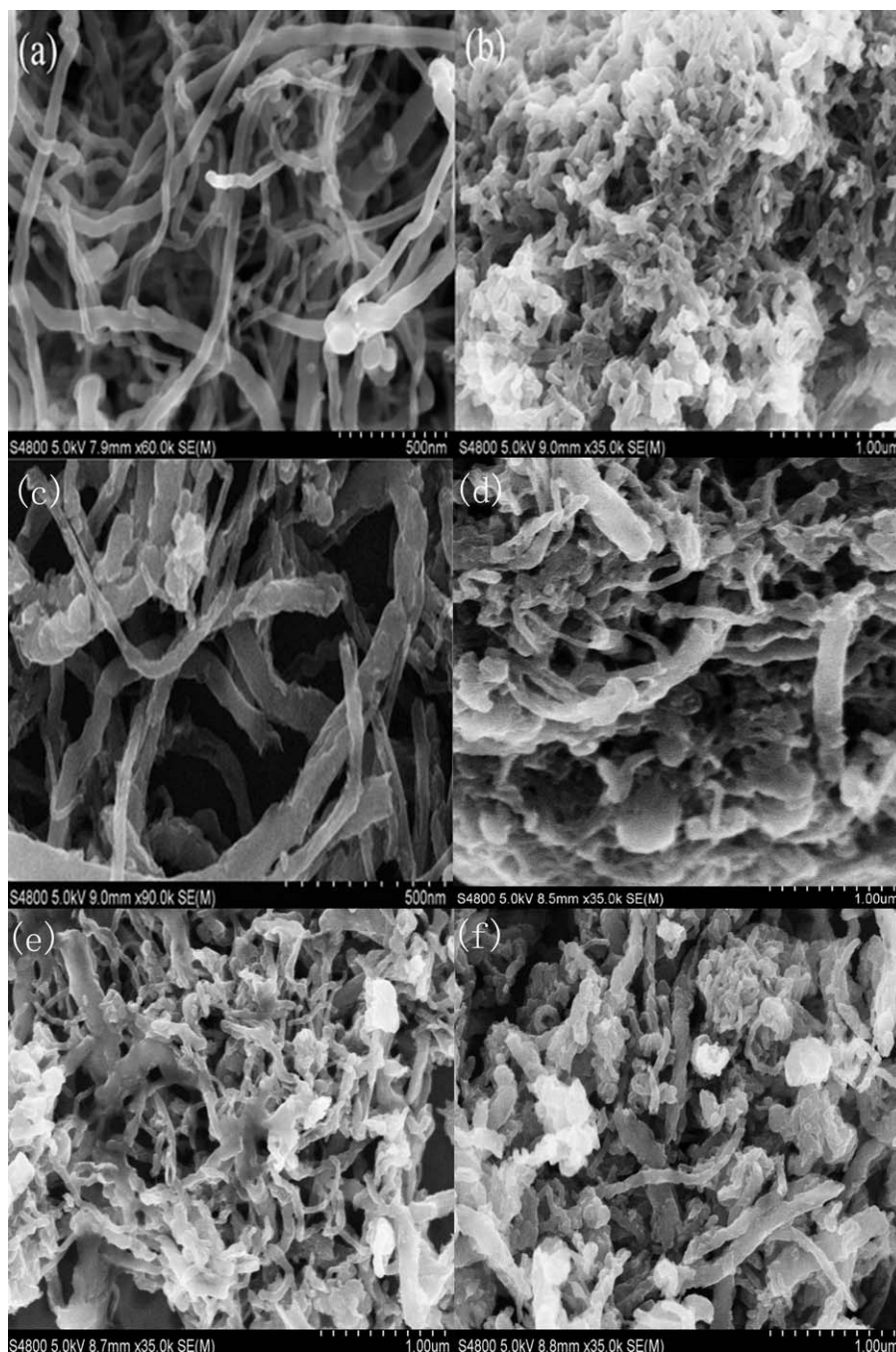


Figure 1. SEM images of (a) MWCNTs, (b) PANI, (c) TCN, (d) PANI/TCN 2-8, (e) PANI/TCN 5-5, and (f) PANI/TCN 8-2.

current than pure TCN. These verify that TCN can greatly improve the electrochemical capacitance and CV symmetry of PANI. Figure 4(b) shows the CV curves of PANI/TCN 8-2 at different scan rates. With the increase of scan rate, the CV curve becomes more and more expand. The CV curve of PANI/TCN 8-2 is still rectangle-like even at a scan rate of 100 mV s^{-1} . This indicates a very quick charge–discharge process in PANI/TCN 8-2 and good capacitance behavior of the composite.

Figure 5 shows galvanostatic charge–discharge curves of different electrode materials at a current density of 2 A g^{-1} . The

galvanostatic charge–discharge curve of TCN is quite symmetric and linear, which indicates good capacitance performance of TCN. It is remarkable that PANI could be nearly considered as resistance from -0.2 to 0.2 V , which means that the potential response of PANI as supercapacitors electrode material is very narrow. This will seriously affect the energy density and power density of PANI.^{36,37} Whereas the linear galvanostatic charge–discharge curve of composites show that they have good electron transport path for the electrolyte ion and electron in the electrode from -0.2 to 0.8 V , which is very favorable for supercapacitors materials.

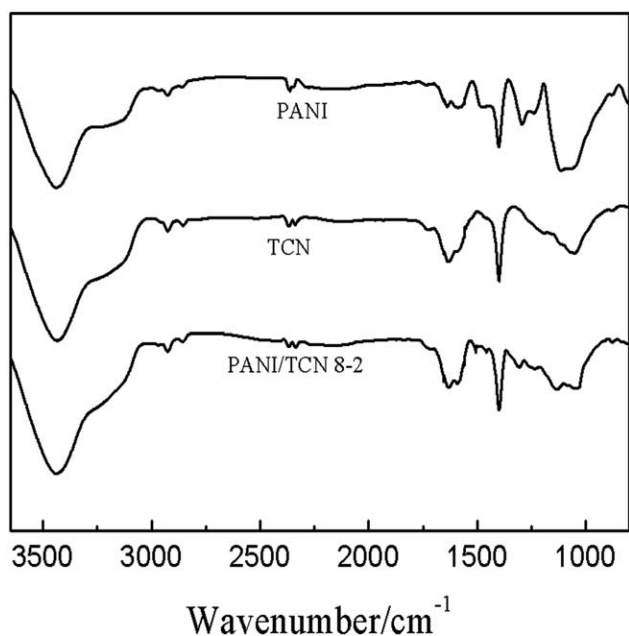


Figure 2. FTIR spectra of PANI, TCN, and PANI/TCN 8-2 materials in KBr pellet.

The gravimetric capacitance of material can be calculated according to the following equation:

$$C = \frac{It}{mV} \quad (1)$$

where C is the specific capacitance of the active material ($F g^{-1}$), I is the constant discharge current (A), t is the discharge time (s), V is the voltage difference in discharge (V), and m is the mass of the active material in a single electrode (g). According to eq. (1), the specific capacitances of TCN, PANI/TCN 2-8, PANI/TCN 5-5, PANI/TCN 8-2, and PANI are 100.02, 165.4, 186.54, 297.72, and 240.02 $F g^{-1}$, respectively, at a current density of 2 $A g^{-1}$. It shows that the specific capacitance

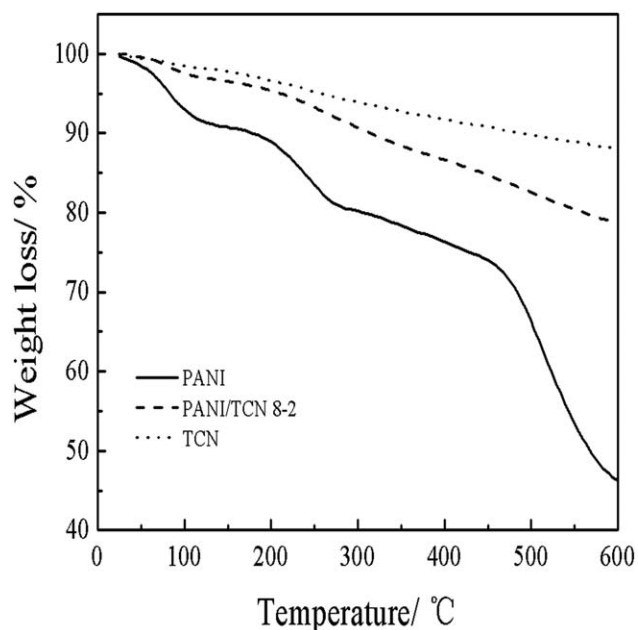


Figure 3. TGA curves of PANI, PANI/TCN 8-2, and TCN (heating rate = $10^{\circ}C min^{-1}$ under a nitrogen atmosphere).

of these composites is a function of the quality ratio of aniline to TCN. When the ratio increases, the specific capacitance increases. The PANI/TCN 8-2 has the highest specific capacitance, which is even higher than PANI at 2 $A g^{-1}$.

The specific capacitance is shown as a function of the current density in Figure 6. With the increase of current density, specific capacitance of materials will decrease. At 0.5 $A g^{-1}$, the specific capacitances of PANI/TCN 8-2, PANI/TCN 5-5, PANI/TCN 2-8, PANI, and TCN are 373.5, 247.4, 220.6, 324, and 130.2 $F g^{-1}$, respectively. From 0.5 to 10 $A g^{-1}$, the specific capacitances of PANI/TCN 8-2, PANI/TCN 5-5, PANI/TCN 2-8, PANI and TCN retain 69%, 63%, 62%, 58% and 63%, respectively. Even at the high current density of 10 $A g^{-1}$, the specific capacitance of

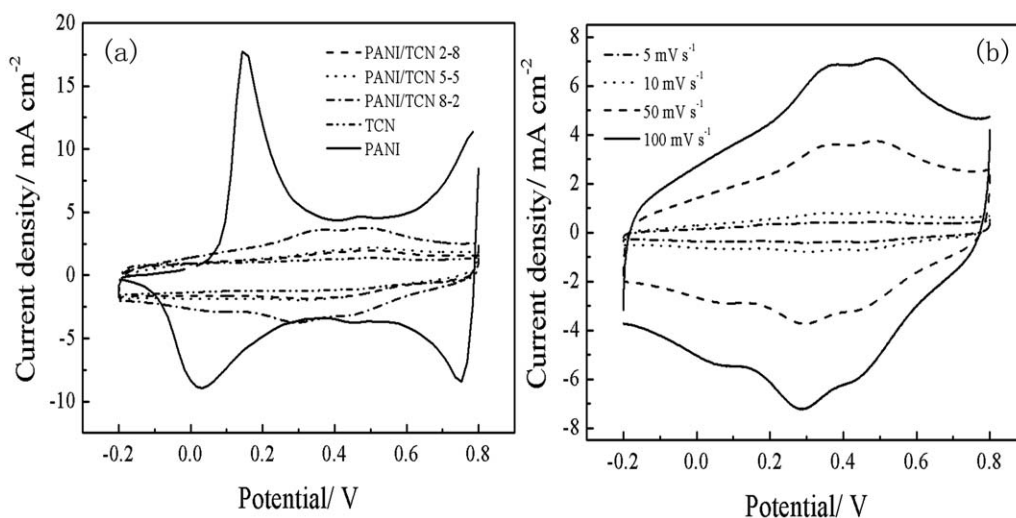


Figure 4. (a) Cyclic voltammograms of PANI, TCN, PANI/TCN 2-8, PANI/TCN 5-5, and PANI/TCN 8-2 at a scan rate of $50 mV s^{-1}$ and (b) cyclic voltammograms of PANI/TCN 8-2 at different scan rates.

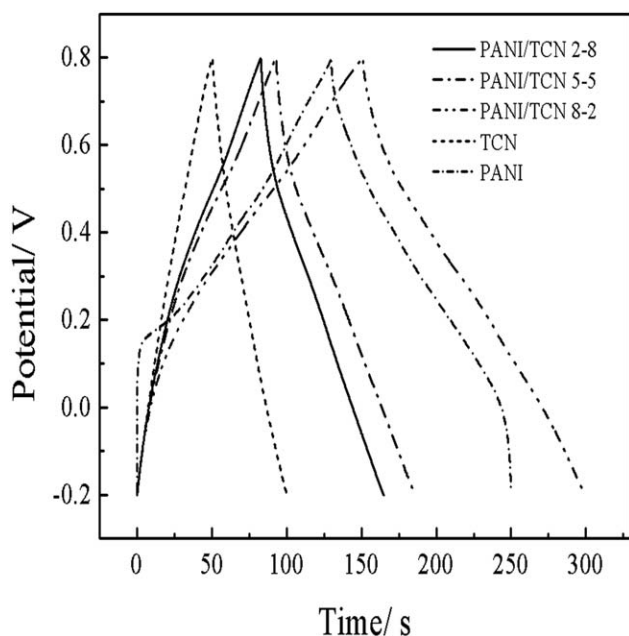


Figure 5. Charge–discharge curves of different electrode materials at a current density of 2 A g^{-1} .

PANI/TCN 8-2 is as high as 257.5 F g^{-1} . It means that the PANI/TCN 8-2 has good electrochemical property with not only high specific capacitance but also good stability at high current density. The high specific capacitance of PANI/TCN 8-2 could be attributed to the synergy of PANI and TCN. All of these indicate that PANI/TCN 8-2 composite is a promising electrode material for high power supercapacitors.

Figure 7 shows the Ragone plots of composites, PANI and TCN. The energy density and power density are calculated from galvanostatic charge–discharge curves at different current densities according to the following equations:

$$E = \frac{1}{2} CV^2 \quad (2)$$

$$P = \frac{E}{t} \quad (3)$$

where E is the energy density (W h kg^{-1}), C is the specific capacitance of the active material (F g^{-1}), V is the voltage difference (V), P is the power density (kW kg^{-1}), t is the discharge time (s). According to eqs. (2) and (3), the energy density of PANI/TCN 8-2 is much higher than those of PANI/TCN 5-5, PANI/TCN 2-8, PANI, and TCN at the same power density, and it reduced slowly with the increase of power density. The maximum energy density of PANI/TCN 8-2 reaches 51.9 W h kg^{-1} based on the total mass of active materials at a power density of 0.5 kW kg^{-1} , and it still remains 35.8 W h kg^{-1} at a power density of 10 kW kg^{-1} , exhibiting an excellent rate capacity. The energy density of composites increases with the increase of the PANI/TCN ratio in composite. Moreover, the energy density of PANI/TCN 8-2 is still higher than that of pure PANI at the same power density.

The cycling electrochemical stabilities of the electrode materials were examined by long-term cyclic voltammetry at 50 mV s^{-1} . The specific capacitance can be calculated according to the following equation and the results are shown in Figure 8:

$$C = \frac{1}{s \cdot m \cdot V} \int_{V_0}^{V_0+V} IdV \quad (4)$$

where C is the specific capacitance (F g^{-1}), V_0 is the voltage of the CV curve (V), and I denotes the response current (A), s is

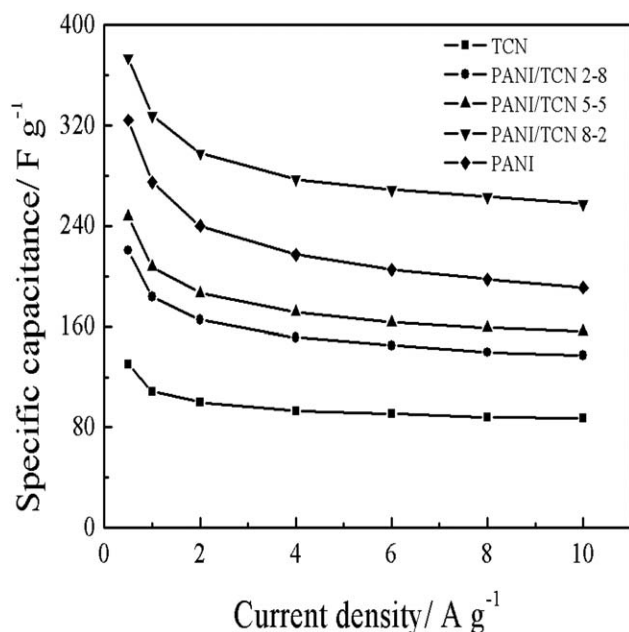


Figure 6. Specific capacitances of PANI, TCN, PANI/TCN 2-8, PANI/TCN 5-5, and PANI/TCN 8-2 at different current densities from 0.5 to 10 A g^{-1} in $1 \text{ M H}_2\text{SO}_4$.

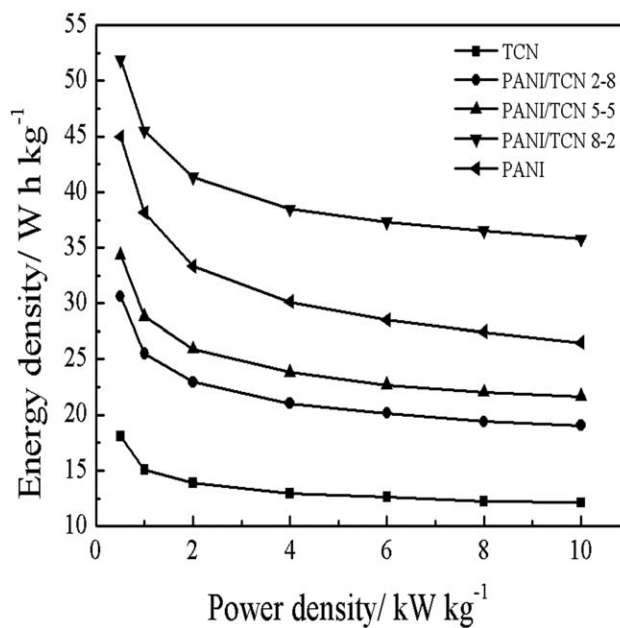


Figure 7. Ragone plots of PANI, TCN, PANI/TCN 2-8, PANI/TCN 5-5, and PANI/TCN 8-2.

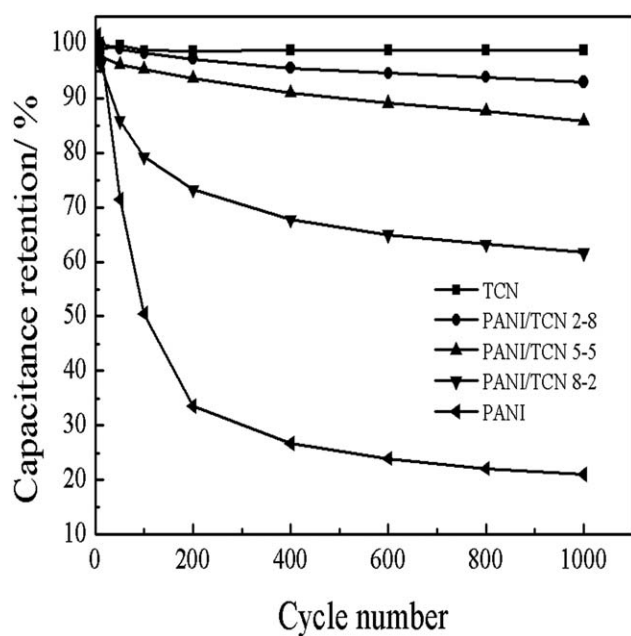


Figure 8. Cycling stability measurement of composites, TCN and pure PANI at 50 mV s^{-1} .

the potential scan rate (mV s^{-1}), V is the potential drop of the CV curve (V), and m is the mass of the active material (g). The specific capacitances of TCN, PANI/TCN 2-8, and PANI/TCN 5-5 retain 98.8%, 93%, and 86%, respectively, after 1000 cycles. The excellent cycling stabilities of PANI/TCN 2-8 and PANI/TCN 5-5 are attributed to the large amount of TCN component in composite. It was seen that the pure PANI only retains 20% of the initial value after 1000 cycles. This is mainly owing to the PANI electrode undergoes swelling, shrinking, creaking, and breaking during the doping/dedoping process. The PANI/TCN 8-2 can keep 61.7% of the initial value after 1000 cycles, indicating that a small amount of TCN can greatly improve cycling stability of the composite. The good cycling stability of PANI/TCN 8-2 composite is mainly because of the synergic effect of both components. The conductive TCN that act as a framework for sustaining PANI, can prevent PANI from severe swelling and shrinking during cycling, and the polymer provides a higher pseudocapacitance because of the redox transition of its different states. Compared with pure PANI, the PANI/TCN has not only higher specific capacitance at high current density but also better cyclic life.

CONCLUSIONS

In summary, PANI/TCN composite was prepared by in situ polymerization of aniline in the presence of TCN. Compared to pure PANI, higher specific capacitance and better cycling stability are achieved for the PANI/TCN 8-2 composite. The highest specific capacitance of 373.5 F g^{-1} is obtained by PANI/TCN 8-2 at 0.5 A g^{-1} . The maximum energy density of PANI/TCN 8-2 reaches 51.9 W h kg^{-1} based on the total mass of active materials at a power density of 0.5 kW kg^{-1} . The specific capacitance of PANI/TCN 8-2 retains 61.7% after

1000 cycles at a scan rate of 50 mV s^{-1} . In a word, after modified by 20 wt % TCN, PANI has higher specific capacitance, higher energy density, wider range of conducting potential, and longer cyclic life.

ACKNOWLEDGMENTS

This work was supported by National Natural Science Foundation of China (Grant No. 51071067, 21271069, J1210040, 51238002) and Science and Technology Program of Hunan Province (2013GK3015).

REFERENCES

- Wang, H.; Casalongue, H. S.; Liang, Y.; Dai, H. *J. Am. Chem. Soc.* **2010**, *132*, 7472.
- Subramanian, V.; Zhu, H.; Vajtai, R.; Ajayan, P. M.; Wei, B. *J. Phys. Chem. B* **2005**, *109*, 20207.
- Wei, W.; Cui, X.; Mao, X.; Chen, W.; Ivey, D. G. *Electrochim. Acta* **2011**, *56*, 1619.
- Huang, Y.; Liang, J.; Chen, Y. *Small* **2012**, *8*, 1805.
- Wang, G.; Zhang, L.; Zhang, J. *Chem. Soc. Rev.* **2012**, *41*, 797.
- Burke, A. *J. Power Sources* **2000**, *91*, 37.
- Frackowiak, E. *Phys. Chem. Chem. Phys.* **2007**, *9*, 1774.
- Guan, C.; Li, X.; Wang, Z.; Cao, X.; Soci, C.; Zhang, H.; Fan, H. *J. Adv. Mater.* **2012**, *24*, 4186.
- Cheng, Q.; Tang, J.; Ma, J.; Zhang, H.; Shinya, N.; Qin, L. *Carbon* **2011**, *49*, 2917.
- Shi, W.; Zhu, J.; Sim, D. H.; Tay, Y. Y.; Lu, Z.; Zhang, X.; Sharma, Y.; Srinivasan, M.; Zhang, H.; Hng, H. H. *J. Mater. Chem.* **2011**, *21*, 3422.
- Conway, B. E. *Electrochemical Supercapacitors: Scientific Fundamentals and Technological Applications (POD)*; Kluwer Academic/plenum: New York, **1999**.
- Ryu, K. S.; Kim, K. M.; Park, N.; Park, Y. J.; Chang, S. H. *J. Power Sources* **2002**, *103*, 305.
- Wang, Q.; Li, J.; Gao, F.; Li, W.; Wu, K.; Wang, X. *New Carbon Mater.* **2008**, *23*, 275.
- Frackowiak, E.; Khomenko, V.; Jurewicz, K.; Lota, K.; Beguin, F. *J. Power Sources* **2006**, *153*, 413.
- Hsieh, C.; Teng, H. *Carbon* **2002**, *40*, 667.
- Wang, K.; Wang, Y.; Wang, Y.; Hosono, E.; Zhou, H. *J. Phys. Chem. C* **2008**, *113*, 1093.
- Frackowiak, E.; Delpeux, S.; Jurewicz, K.; Szostak, K.; Cazorla-Amoros, D.; Beguin, F. *Chem. Phys. Lett.* **2002**, *361*, 35.
- Vivekchand, S.; Rout, C. S.; Subrahmanyam, K. S.; Govindaraj, A.; Rao, C. *J. Chem. Sci.* **2008**, *120*, 9.
- Yan, J.; Wei, T.; Shao, B.; Fan, Z.; Qian, W.; Zhang, M.; Wei, F. *Carbon* **2010**, *48*, 487.
- Liu, H.; Wang, Y.; Gou, X.; Qi, T.; Yang, J.; Ding, Y. *Mater. Sci. Eng. B* **2012**, *178*, 293.
- Zhou, Y.; He, B.; Zhou, W.; Huang, J.; Li, X.; Wu, B.; Li, H. *Electrochim. Acta* **2004**, *49*, 257.

22. Wu, M.; Snook, G. A.; Gupta, V.; Shaffer, M.; Fray, D. J.; Chen, G. Z. *J. Mater. Chem.* **2005**, *15*, 2297.
23. Zhou, Y.; Qin, Z.; Li, L.; Zhang, Y.; Wei, Y.; Wang, L.; Zhu, M. *Electrochim. Acta* **2010**, *55*, 3904.
24. Gupta, V.; Miura, N. *J. Power Sources* **2006**, *157*, 616.
25. Sivakkumar, S. R.; Kim, W. J.; Choi, J. A.; MacFarlane, D. R.; Forsyth, M.; Kim, D. W. *J. Power Sources* **2007**, *171*, 1062.
26. Meng, C. Z.; Liu, C. H.; Fan, S. S. *Electrochem. Commun.* **2009**, *11*, 186.
27. Wang, K.; Zhao, P.; Zhou, X. M.; Wu, H. P.; Wei, Z. X. *J. Mater. Chem.* **2011**, *21*, 16373.
28. Wang, Y.; Zhang, J.; Zang, J.; Ge, E.; Huang, H. *Corros. Sci.* **2011**, *53*, 3764.
29. Jiao, L.; Zhang, L.; Wang, X.; Diankov, G.; Dai, H. *Nature* **2009**, *458*, 877.
30. Kosynkin, D. V.; Higginbotham, A. L.; Sinitskii, A.; Lomeda, J. R.; Dimiev, A.; Price, B. K.; Tour, J. M. *Nature* **2009**, *458*, 872.
31. Kosynkin, D. V.; Lu, W.; Sinitskii, A.; Pera, G.; Sun, Z.; Tour, J. M. *ACS Nano* **2011**, *5*, 968.
32. Wang, H.; Wang, Y.; Hu, Z.; Wang, X. *ACS Appl. Mater. Interfaces* **2012**, *4*, 6827.
33. Saini, P.; Choudhary, V.; Singh, B. P.; Mathur, R. B.; Dhawan, S. K. *Mater. Chem. Phys.* **2009**, *113*, 919.
34. Chen, H.; Müller, M. B.; Gilmore, K. J.; Wallace, G. G.; Li, D. *Adv. Mater.* **2008**, *20*, 3557.
35. Ding, L.; Wang, X.; Gregory, R. V. *Synthetic Met.* **1999**, *104*, 73.
36. Demarconnay, L.; Raymundo-Pinero, E.; Beguin, F. *J. Power Sources* **2011**, *196*, 580.
37. Zhang, W.; Ma, C.; Fang, J.; Cheng, J.; Zhang, X.; Dong, S.; Zhang, L. *RSC Adv.* **2013**, *3*, 2483.